PHYSICAL REVIEW B VOLUME 25, NUMBER 2 15 JANUARY 1982

Phenomenology of solid solubilities and ion-implantation sites: An orbital-radii approach

Vijay A. Singh and Alex Zunger
Solar Energy Research Institute, Golden, Colorado 80401
and Department of Physics, University of Colorado, Boulder, Colorado 80309
(Received 18 May 1981)

The crossing points of the first-principles nonlocal screened atomic pseudopotentials of the elements were shown previously to constitute a sensitive anisotropic atomic-size scale. This scale allows systematization of the crystal structure of as many as 565 binary compounds [A. Zunger, Phys. Rev. B 22, 5839 (1980)]. In this paper we apply the same coordinates for systematizing the trends in the solid solubilities in the divalent solvents Be, Mg, Zn, Cd, Hg, and in the semiconductor solvents Si and Ge (192 data points), as well as the location of the ion-implantation sites in Be and Si (60 data points). We find that these *nonempirical* and *atomic* coordinates produce a systematization of the data that overall is equal to or better than that produced by the *empirical* coordinates of Miedema and Darken-Gurry which are derived from properties of the *condensed* phases. Furthermore, it is found that the orbital-radii coordinates which incorporate directly the effects of only the s and p atomic orbitals are capable of predicting the solubility trends and ion-implantation sites even for the (nonmagnetic) transition atom impurities.

I. INTRODUCTION

No element can be totally purified. Impurities are always present. In a semiconductor such as silicon, the presence of an impurity may enhance (e.g., phosphorus) or degrade (e.g., a transition element) its technological property. In the case of metals, impurities may alter mechanical properties such as elasticity and ductility. Whether a given impurity is substitutional, interstitial, or at all soluble in a host is a question of considerable interest in fields as varied as metallurgy and modern semiconductor technology.

Many attempts have been made so far to answer this question. For metals, Hume-Rothery rules[1] and Darken-Gurry plots[2–4] have been popular for decades. Recently, Chelikowsky[5] applied the Miedema parameters[6] to the study of solid solubilities in divalent metal hosts. Alonso and Simozar[7] modified this scheme for the study of solubility in Fe and Co. These schemes are empirical. It would be of great interest to study such trends using parameters derived from a first-principles quantum-mechanical calculation. Such a scheme, if successful, would constitute a bridge between the largely abstract field of quantum mechanics and the highly applied field of semiconductor technology.

Recently first-principles atomic nonlocal pseudopotential calculations were carried out[8] for 70 elements of the Periodic Table. From the crossing points of these nonlocal pseudopotentials, orbital radii were constructed and applied by one of us to predict the structural characteristics of 565 binary alloys.[8] In this paper we demonstrate that the same orbital radii yields a graphical prediction of solid solubilities in Be, Mg, Zn, Cd, Hg, Si, and Ge, as well as the sites of ions implanted in Be and Si with an accuracy comparable to (or better than) the empirical coordinates.[2–5]

II. SOLID SOLUBILITY

A. Data and its trends

The success or failure of various phenomenological models predicting solubilities depends to a large extent on the rather arbitrary definition of the critical solute concentration X_c above which the solute is said to be "soluble". In general, the larger the chosen X_c, the easier it is to find a model predicting successfully which elements will be soluble in a given host. The classical approach to solubilities by Darken and Gurry[2] and Waber *et al.*[3] defines $X_c = 5-15$ at. %; Alonso and Simozar[7] have used

$X_c = 1$ at. %, while Chelikowsky[5] has used $X_c = 0.5$ at. %. To provide a finer distinction and at the same time impose a more stringent test on the model, we use $X_c = 0.01$ at. %. Furthermore, the success of various solubility models also depends critically on the temperature T_s at which $X_c(T_s)$ is measured. Early models[2,3] often used data with T_s at or above the solute melting temperature; Alonso and Simozar[7] chose T_s near the solute melting point, whereas Chelikowsky[5] used $T_s \simeq 300$ K. We follow the latter choice because it constitutes in most cases a more severe test of the model. The experimental data for solubilities above or below $X_c = 0.01$ at. % and $T_s \simeq 300$ K was taken from Refs. 5 and 9–11. A typical set of data is shown in Fig. 1 for Si.[11] While a complete theory of solid solubility should explain the entire curves $X_c(T_s)$ for all hosts and solutes, we will attempt here to merely describe phenomenological models that predict which elements will be soluble or insoluble in a given host to the extent X_c at a temperature T_s. Figure 1 clearly demonstrates the need to specify X_c and T_s: While for $T_s = 1100$ °C and $X_c = 15$ at. % none of the elements included in Fig. 1 is soluble in Si, for $X_c = 1$ at. %, As and B are soluble and for $X_c = 0.01$ at. % P, Sn, Sb, Ga, Li, and Al are soluble as well. The pronounced curvatures of the solubility lines in Fig. 1 also suggest the importance of specifying T_s.

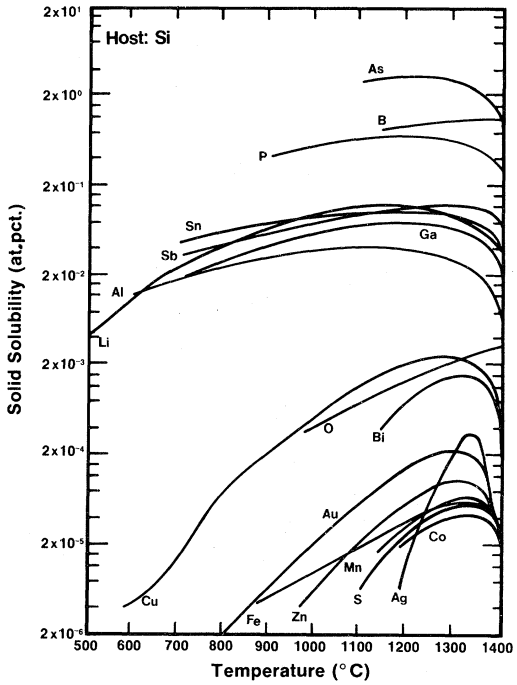

FIG. 1. Experimental solid solubilities in silicon (Ref. 11).

A typical set of data, collected from published phase diagrams[9–11] is shown in Table I for the hosts Be, Mg, Zn, Cd, Hg, Si, and Ge and for impurities belonging to the first five rows of the Periodic Table. The plus and minus signs in the solubility matrix $S(H,I)$ denote (H=host, I=impurity or solute), respectively, soluble and insoluble impurities to the extent $X_c = 0.01$ at. % at room temperature (or the closest available temperature, as indicated). Inspection of this data suggests immediately a number of striking regularities. These include: (i) All noble metals Cu, Ag, and Au are soluble in *all* the divalent hosts but insoluble in silicon and germanium. (ii) The IIIA elements Al, Ga, In, and Tl, are soluble in all of the heavy divalent hosts Mg, Zn, Cd, and Hg (with the exception of Tl in Zn data which seems irregular) as well as in silicon. (iii) The alkali elements Li, Na, K, Rb, and Cs are all soluble in mercury but insoluble in magnesium (with the exception of Li), although Mg and Hg have nearly identical atomic radii (3.34 and 3.35 a.u., respectively). (iv) Silicon and germanium are insoluble in all of the divalent hosts, whereas the larger Sn atom is mostly soluble in these hosts. [In Ref. 5, Ge was indicated to be soluble in Cd, violating the trend indicated here. We find, however (Ref. 10, p. 311), that Ge is in fact insoluble in Cd.] (v) For the solutes measured in these hosts, Be is best able to dissolve transition atoms (60%), whereas in Zn, Cd, and Hg, about 10% of the soluble elements are transition atoms.

In the ion-implantation data, one similarly finds intriguing features: *large* ions such as Pb, K, Rb, and Cs (atomic radii of 3.6, 4.86, 5.2, and 5.6 a.u., respectively) often take *substitutional* sites in Si (atomic radius of 3.2 a.u.). Similarly, for many of the interstitial implants (e.g., I and Xe in Be), one finds that the sum of the implant and host atomic radii far exceeds the crystallographic touching-sphere bond distance.[5] Clearly,[5] the simplistic view of packing of "hard touching spheres" often used in crystallography does not hold for (metastable) implantation.

The phenomenological models introduced below will not explain all of these regularities. They do, however, go a long way in systematizing most of the trends apparent in Table I. We describe in Sec. II B the various phenomenological models attempting to organize the solubility matrix $S(H,I)$.

TABLE I. Experimental solubilities in Be, Mg, Zn, Cd, Mg, and Si (Refs. 5 and 9–11), and the lattice location of ion-implanted impurities in Be (Ref. 23) and Si (Ref. 24). The signs + and − denote soluble and insoluble elements, respectively. The solubilities are taken from data at (or extrapolated to) room temperature $T_s=300$ K for all solvents, except Si and Ge for which the data is measured at $T_s=1250$ and 900 K, respectively. For ion-implanted sites: *S*, substitutional; *O*, octahedral; *T*, tetrahedral; *I*, interstitial; *R*, random; *D*, defect association.

	Host								Host							
Impurity	Be	Mg	Zn	Cd	Hg	Si	Ge	Impurity	Be	Mg	Zn	Cd	Hg	Si	Ge
Li	*S*	+	−	+	+	*I,R*	+ −	N						*R*	+
Na		−			+	*I*		P						*S*	
K		−			+			As	*O*	−			−	*S,D*	+ +
Rb		−			+	*R*		Sb	*O*	−		−	−	*S*	+ +
Cs	*O*	−			+	*R*		Bi	*O* −	+	−	+	+	*S*	− −
Cu	*S* +	+	+	+	+	−	−	Sc		+					
Ag	*S* +	+	+	+	+	−	−	Y		+	−				
Au	*S* +	+	+	+	+	*S,I*	− −	La		+			+		
Be	*	−			−		+	Ti	*T*	+	−		−		
Mg	−	*	+	+	+			Zr		+	−		−	*I*	
Ca	−	+			+			Hf	*T*	−				*I*	
Sr		+			+										
Ba	*O* −	−		−				V	*T* −				−		
								Nb		−					
Zn	*S* −	+	*	+	+	*I*	− −	Ta	*T*						
Cd	*T* −	+	+	*	+	*I*	− −								
Hg	*O*	+	+	+	*	*S,I*	−	Cr	+		+		−		
								Mo	*T*		−		−		
B	*S,R*					*S*	+	W	*T*	−	−		−		
Al	*I* +	+	+		+		+ +								
Ga	*O* −	+	+	+	+	*S,I*	+ +	Mn		+	+		−		−
In	*T*	+	+	+	+	*S,I*	− −	Tc				−			
Tl	*O*	+	−	+	+	*S,I*		Re	−		−				
C							+	Fe	*S* +	−	−	−	−	*I*	− −
Si	−	−	−	−	−		*	Ru							
Ge	*O* −	−	−	−	−		*	Os	*S* −						
Sn	−	+	+	+	+	*S*	+ +								
Pb	*O*	+	−	+	+	*S*	−	Co	*S* +	−	−	−	−	*I*	− −
								Rh							
O			−					Ir							
S							−								
Se						*S*		Ni	*S* +		−	−	−		− −
Te						*S*	−	Pd	*S* +	+	−	−			−
								Pt	*S* +		−		+		
I	*O*														
Xe	*O*					*R,S*									
Ne	*I*														
								Totals	23	38	29	22	37	24	19

B. Phenomenology of solid solubility

A number of phenomenological models have previously been attempted for predicting whether given elements will be soluble (to an extent X_c at temperature T_s) in various host crystals. Largely, these models are diagrammatic in nature. They are often based on the definition of dual coordinate systems $R_1(I,H)$ and $R_2(I,H)$, which defines two scales by which some chosen physical characteristics of the impurity (I) and host (H) are measured. One then attempts to find in the $R_1(I,H)$ vs

$R_2(I,H)$ plane for a given host crystal two nonoverlapping and internally connected domains corresponding to soluble and insoluble impurities. A successful choice of the scales $R_1(I,H)$ and $R_2(I,H)$ results in a small number of misplaced solutes (i.e., soluble element residing in the domain of insoluble elements or vice versa) and can hence be used as both a systematizing and a predictive tool.

We note that in solid-state physics and chemistry there are numerous classical phenomenological models attempting to systematize predictively some observed physical property $S_{\rm obs}(A,B)$ of binary AB systems in terms of general *linear dual coordinate systems* $R_1(A,B)$ and $R_2(A,B)$. One model is, for example, the Mooser-Pearson[12] model for classifying the crystal structure of the stoichiometric octet AB compounds in terms of the atomic electronegativity and the principal valence quantum number for elements A and B. Similarly, the empirical pseudopotential method[13] permits one to express the optical band gap of binary AB semiconductors in terms of the atomic pseudopotential form factors of atoms A and B. Miedema's scheme[6] for predicting the signs of the heats of formation ΔH_f of binary AB alloys attempts the organization of the matrix $S_{\rm obs}(A,B)\equiv\Delta H_f(A,B)$ in terms of the chemical potential (related to the elemental solid work function) and the Wigner-Seitz cell boundary charge density of the pure solid element. A quantum-mechanical dual coordinate scale is provided by the Phillips—Van Vechten optical dielectric electronegativity[14] in terms of the homopolar and ionic band gaps. In the orbital radii (OR) scale[15] the different crystal structures of all binary AB crystals have been systematized[8] through the coefficients

$$R_1^{\rm OR}(A,B)\equiv R_\pi(A,B)=|r_p^A-r_s^A|+|r_p^B-r_s^B|$$

and (1)

$$R_2^{\rm OR}(A,B)\equiv R_\sigma(A,B)=|(r_p^A+r_s^A)-(r_p^B+r_s^B)|\ ,$$

where r_s^i and r_p^i are the crossing points for the screened atomic pseudopotentials for angular momental $l=0$ and $l=1$, respectively, of atom i.[16,17]

One often encounters in structural chemistry and solid-state physics, single (rather than dual) scales. Such are the scales of orbital promotion energy[18] and the valence electron concentration per atom[1] used to systematize some classes of crystal structures. It is clear, however, from the available solid solubility data (see cf. Table I) that no such simple single scale can successfully delineate soluble from insoluble elements. For example, considering Mg (see Table I) as a host, one finds small but insoluble elements such as Be (atomic radius of 2.35 a.u., ionic radius of 0.57 a.u., compared to the values for Mg of 3.34 and 1.23 a.u., respectively) and large but soluble elements such as Ca and Sr (atomic radii of 4.2 and 4.49 a.u., ionic radii of 1.73 and 2.08 a.u., respectively). One similarly finds electronegative but insoluble elements (Be with a Pauling electronegativity of 1.5 compared with 1.2 for Mg) as well as electropositive but soluble elements (Ca and Sr with an electronegativity of 1.0). Clearly, the impurity size or electronegativity, considered separately, cannot in general delineate solid solubilities. Similarly, one might have hoped to delineate soluble from insoluble impurities according to whether the impurity atomic potential is attractive or repulsive with respect to that of the host (i.e, donorlike versus acceptorlike character). Using the first-principles atomic pseudopotentials[16] as a guide, one finds, however, that Si, Co, Fe, W, As, Ge, and Sb are attractive impurities in Mg, yet they are insoluble, whereas Li, Ca, and Sr are repulsive impurities but soluble. The heat of formation of the binary HI compound is likewise an insufficient coordinate to delineate soluble from insoluble elements: One often finds insoluble impurities I that form stable binary compounds with the host H (i.e., negative heat of formation). Few such examples are HgMn ($B2$); HgTi ($L1_0$); CdBa ($B2$); ZnNi, ZnTi, ZnY, and ZnZr (all $B2$); ZnLi ($B32$); and ZnPd and ZnPt ($L1_0$). (The first symbol refers to the host while the second refers to the impurity that is insoluble in that host, and in parentheses, the crystallographic symbol identifies the crystal structure of the HI compound.[8]) In contrast to these unsuccessful single solubility coordinates, dual scales can, however, effect a reasonable separation of soluble from insoluble impurities.

Dual scales can be divided into two categories: those that are invariant with respect to the identity of the host crystals, and those that are not. In the first category (referred to as "host invariant scales") we find two models—the Darken-Gurry[2] and Chelikowsky[5] models. The Darken-Gurry[2] (DG) scale attempts to separate soluble from insoluble elements using

$$R_1^{\rm DG}(I)=R_I^{\rm CN12}$$

and (2)

$$R_2^{\rm DG}(I)=X_I\ ,$$

where R_I^{CN12} represents the 12-coordinated Goldschmidt radii, and X_I is the electronegativity of the impurity atom I. Similarly, Chelikowsky[5] (C) has recently provided a separation of solid solubilities using

$$R_1^C(I)=n_I^{*1/3}$$

and (3)

$$R_2^C(I)=\phi_I^* ,$$

where ϕ_I^* and $n_I^{*1/3}$ are Miedema's[6] parameters for the impurity elements.

Underlying the Darken-Gurry scheme are the empirical Hume-Rothery[1] rules, which state that solid solubilities are encouraged by a small difference in atomic sizes between the solute and solvent [i.e., $|R_1^{DG}(I)-R_1^{DG}(H)|$] and a sufficiently large (but not too large) electronegativity difference [i.e., $|R_2^{DG}(I)-R_2^{DG}(H)|$]. The first factor minimizes the elastic strain attendant upon introducing an impurity into the host, while the second factor enhances the electrostatic stabilization of the system through charge transfer. Underlying the Chelikowsky scheme is the Miedema model for compound heats of formation.[6] This model successfully predicts the sign of the heat of formation $\Delta H_f(H,I)$ of the binary 50%-50% alloys in terms of a destabilizing factor $[R_1^C(I)-R_1^C(H)]^2$ measuring the energy spent to overcome the mismatch in the Wigner-Seitz cell boundary charge density, and a stabilizing factor $[R_2^C(I)-R_2^C(H)]^2$ measuring the energy released upon electron transfer. Since elemental work functions correlate well with atomic electronegativities,[7] the DG and C schemes share the coordinates $R_2^{DG} \propto R_2^C$. Both models use empirical quantities defined from the properties of the condensed phases ($R_1^{CN12}, n_I{}^{*1/3}, \phi_I^*$) or related molecules ($X_I$). These coordinates are isotropic.

In both the DG and C schemes, the relative locations of the solute elements in the R_1 vs R_2 plot are independent of the identity of the host, simply because the scales R_1 and R_2 are host independent. (Clearly, addition of linear host-dependent constants to these scales does not change the relative orientation of the various points on the plot.) In this sense, such schemes differ from all other host-dependent dual scales (which depend on both A and B). The latter scales are host-dependent either because of the use of nonlinear functional forms $R(A,B)$ or due to the lack of a unique element (i.e., host) in such plots. In host-invariant schemes such as the DG and C, it is then essential to introduce some host-dependent degrees of freedom to specify to which solvent the plot pertains. A predictive prescription like this is essential to these models as is the choice of the scales $R_1(I)$ and $R_2(I)$ themselves.

Such a prescription was provided by Darken and Gurry[2–4] for their scale in Eq. (2); an ellipse or square which is centered at the coordinates of the host atom $R_1^{DG}(H)$ and $R_2^{DG}(H)$ and has one axis of $\pm 15\%$ of the host atomic radius R_H^{CN12} and another axis of ± 0.4 of the host's electronegativity X_H is predicted to include in it only $\{R_1^{DG}(I), R_2^{DG}(I)\}$ values of soluble impurities. Waber *et al.*[3] and Chelikowsky[5] have extensively analyzed the success of the DG scheme and found that it has an overall predictive value of about 80%. The host-invariant Chelikowsky scheme is illustrated graphically in Fig. 2. Plotted are the $R_1^C(I)$ and $R_2^C(I)$ values [Eq. (3)] of numerous impurity atoms I. Chelikowsky noted that most soluble impurities tend to cluster in elliptical domains, shown in Fig. 2 for the hosts Hg (ellipse labeled 1), Cd (curve 2), and Zn (curve 3). However, in this scheme there is

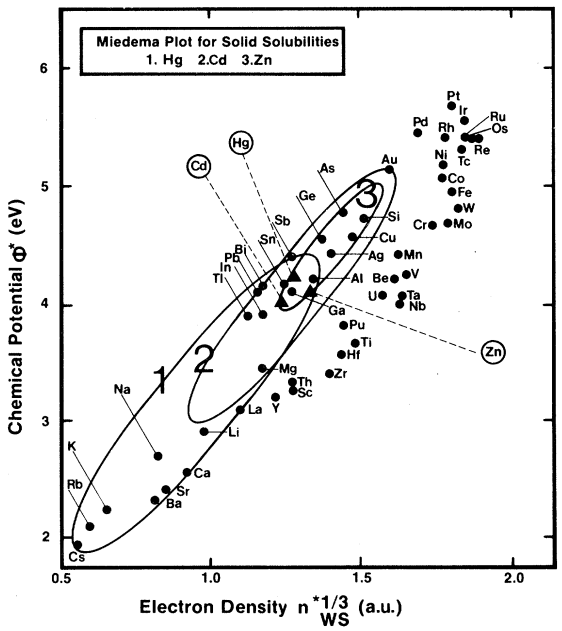

FIG. 2. A Chelikowsky $R_1^C(I)$ vs $R_2^C(I)$ plot for solubilities [Eq. (3)]. All impurity atoms I are denoted by circles enclosing their chemical symbol. The hosts are Hg, Cd, and Zn; their coordinates are indicated by the large full triangles and their chemical symbols identified by the broken lines. The three ellipses enclose the region of predicted solubility [to a level of $X_c=0.5$ at. %, $T_s \simeq 300$ °C (Ref. 5)] for (1) Hg, (2) Cd, and (3) Zn. Note that the coordinates of the hosts (solid triangles) bear no obvious relationship to their home ellipses.

no systematic method that specifies the host-dependent ellipse (i.e., its origin and two radii and the angle they make with the coordinate system). The ellipses are in fact drawn to include in them as many known soluble impurities as possible. It is seen, for example, that the coordinates $R_1^C(H)$ and $R_2^C(H)$ corresponding to the solvent atom (denoted in Fig. 2 as large triangles and identified with dashed lines) bear no obvious relation to their home ellipses: They are clustered at the center of the R_1^C vs R_2^C plane. Using this procedure, however, it was possible[5] to provide a diagrammatic separation of soluble from insoluble impurities, which has a considerably higher degree of success than the Darken-Gurry scale.

Such difficulties encountered with host-invariant procedures can be avoided by schemes using host-dependent coordinates. In such scales the relative positions of various impurities is different for different hosts. Although in such methods one still needs to divide the $R_1(I,H)$ vs $R_2(I,H)$ plane into soluble and insoluble domains, the algorithm need not be explicitly host dependent: it may be, for instance, a minimum-error prescription. Such a scheme was recently provided by Alonso and Simozar[7] (AS), who used

$$R_1^{\mathrm{AS}}(I)=R_I^{\mathrm{WS}}$$

and (4)

$$R_2^{\mathrm{AS}}(I,H)=QR_1^M(I,H)-PR_2^M(I,H)-d(I,H)\ .$$

Here, $R_1^M(I,H)$ and $R_2^M(I,H)$ are the Miedema coordinates[6] where P and Q are constants for certain groups of elements and $d(I,H)$ is another constant which differs from zero only if either I or H is a polyvalent element with p electrons.[6] R_I^{WS} is the Wigner-Seitz radius of element I in its stable crystal structure, related to the observed unit-cell volume per atom Ω_a by $R^{\mathrm{WS}}=(3\Omega_a/4\pi)^{1/3}$ [note that R_I^{WS} is different from the 12-coordinated radius used by Darken and Gurry[2] in Eq. (2); the quantitative differences between these radii can be as large as 10%]. The coordinate $R_2^{\mathrm{AS}}(I,H)$ is equal in the Miedema model to the heat of formation of the 50%-50% binary compound HI (positive or negative).

Underlying the Alonso-Simozar model is the contention that since the Chelikowsky model [Eq. (3)] constitutes an improvement over the Darken-Gurry model [Eq. (2)] but lacks an independent ion-size coordinate (because n_I^* is imperfectly correlated with the inverse atomic volume Ω_a), a combination of the two models might provide a still better separation of solid solubilities. Indeed, when applied to the hosts Fe and Co, it was found[7] that for the critical solubility $X_c=1$ at. % and a T_s below the solute melting point the model works better than the Chelikowsky model: The only errors the model makes, for instance, for Fe as a host are for I=Sn, Sb, As, Ge, and Si (experimentally they are soluble but they appear in the insoluble domain of the R_1^{AS} vs R_2^{AS} plot) and for B (experimentally insoluble but appears in the soluble domain of the plot). If, however, the values of R_I^{WS} for As, Si, and Ge are reduced (by 3%, 10%, and 9%, respectively) to correspond to metallic phases rather than to the stable covalent crystal phases,[6] the only errors made by the model are those for Sb, Sn, and B. Boron is a marginal exception. This is a very high success rate and constitutes a considerable improvement over the Chelikowsky model [errors made for Sn, Sb, B, Ag, Ga, Ta, Nb, and Ti). However, examination of Alonso and Simozar's data points for Fe and Co reveals that a single coordinate $R_1^{\mathrm{AS}}(I)$ is sufficient to provide a separation between soluble and insoluble elements identical to that obtained with their dual scale.[19]

Common to all of the successful phenomenological solubility dual coordinate models [i.e., Eqs. (2)—(4)] are the facts that (i) the elemental coordinates are derived from data on condensed phases (e.g., R_I^{CN12},R_I^{WS},ϕ_I^*,$n_I{}^{*1/3}$), not the properties of the individual atoms, (ii) the coordinates are empirical and largely derived from experiment indirectly; hence, their microscopic significance is often unclear, and (iii) the coordinates are isotropic; i.e., they do not involve directional forces. In Sec. III we examine the predicted solubility diagrams using the l-dependent ("nonlocal") crossing points of the *ab initio* atomic pseudopotentials[8] [Eq. (1)]. These are (i) atomic (rather than solid-state) coordinates, (ii) nonempirical, and (iii) anisotropic. The orbital radii scale is explicitly host dependent, unlike the scales in Eqs. (2) and (3). We attempt here to establish a separation between soluble and insoluble elements (Sec. III) as well as to predict the location of ion-implanted species (Sec. VI) using a *minimum* of two coordinates; the addition of a third coordinate[7] may improve the separation. Our conclusion on the importance of this anisotropy for determining the correct site symmetry in condensed phases supports a similar conclusion by Machlin and Whang[20] drawn from the study of the

$A15$ phases. It also supports the recent findings of Burdett *et al.*[21] who showed that by using the present r_s and r_p coordinates alone, it was possible to predict with 98% accuracy the distribution of normal and inverted spinels (AB_2X_4) over a data base of 172 crystals. In contrast, the pure d-orbital-based crystal-field approach was found[21] to be far less successful in predicting site preferences for spinels.

III. THE ORBITAL RADII APPROACH TO SOLID SOLUBILITIES

The orbital radii[8] $\{r_s^A, r_p^A, r_d^A\}$ of an element A measure the effective *core size* of an atom as sampled by valence electrons of angular momentum s, p, and d, respectively. As such, they depend only weakly on the chemical environment (i.e., are transferrable), they are anisotropic, and they do not invoke a picture of touching hard spheres. They are derived entirely nonempirically for each element (the only input being the atomic number) by mapping the all-electron, local density, single-particle equation into a pseudopotential representation.[8,16,17] Inherent in this mapping are the requirements that such pseudopotentials, when used in variational calculations, accurately reproduce the atomic valence orbital energies, and the valence wave functions in the chemically relevant "tail" region, and that they be transferrable from one chemical environment to the other. The orbital radii $\{r_s^A, r_p^A, r_d^A\}$ are the crossing points of these l-dependent screened atomic pseudopotentials; as such they provide the "fingerprint" of the valence electron properties of the atom encoded into the core. They have been successfully used to systematize the observed crystal structures of 565 binary AB compounds.[8] (See Refs. 16 and 17 for details.) A complete table of $\{r_s, r_p, r_d\}$ for 70 elements is included in Ref. 8, Table I. These values are used unchanged in this work.

We will consider the divalent hosts Be, Mg, Zn, Cd, and Hg studied by Chelikowsky,[5] as well as the four-valent covalent Si and Ge hosts. The divalent hosts produce a symmetric solubility matrix $S(H,I)=S(I,H)$; i.e., Mg, Zn, Cd, and Hg are all mutually soluble, whereas Be is insoluble in these hosts and Mg, Zn, Cd, and Hg are insoluble in Be. This parallels the property of the orbital-radii coordinates $R_\sigma(I,H)=R_\sigma(H,I)$ and $R_\pi(I,H)=R_\pi(H,I)$.

Figures 3(a) and 4–9 present orbital-radii solubility maps for the hosts Be, Mg, Zn, Cd, Hg, Si, and Ge based on the data of Table I. The total of 192 data points are distributed among the hosts Be, Mg, Zn, Cd, Hg, Si, and Ge as follows: 23, 38, 29, 22, 37, 24, and 19, respectively. In the case of di-

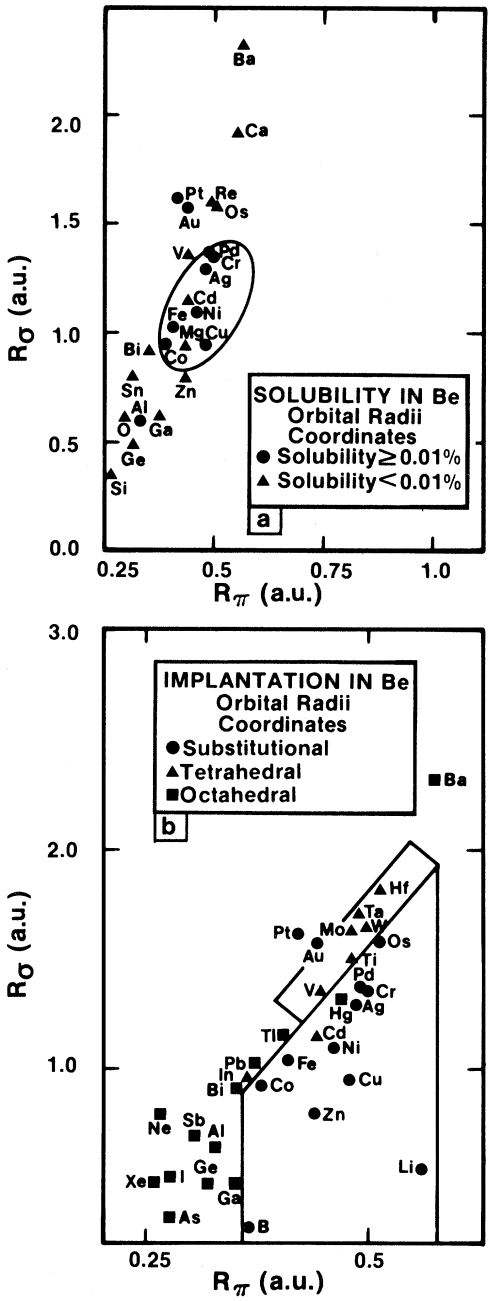

FIG. 3. Solubility (a) and ion-implantation (b) orbital-radii maps for Be. The solubility data is taken at (or extrapolated to) room temperature $T_s=300$ K (Refs. 5, 9, and 10). In Fig. 3(b), Cs falls outside the frame of the figure. It belongs correctly to the octahedral domain.

valent hosts Mg (Fig. 4) and Zn (Fig. 5), for which the present model indicates, respectively, the highest (90% reliability) and lowest (76% reliability) degrees of success, we also present for comparison the corresponding plots using the Chelikowsky coordinates of Eq. (3). For each plot we

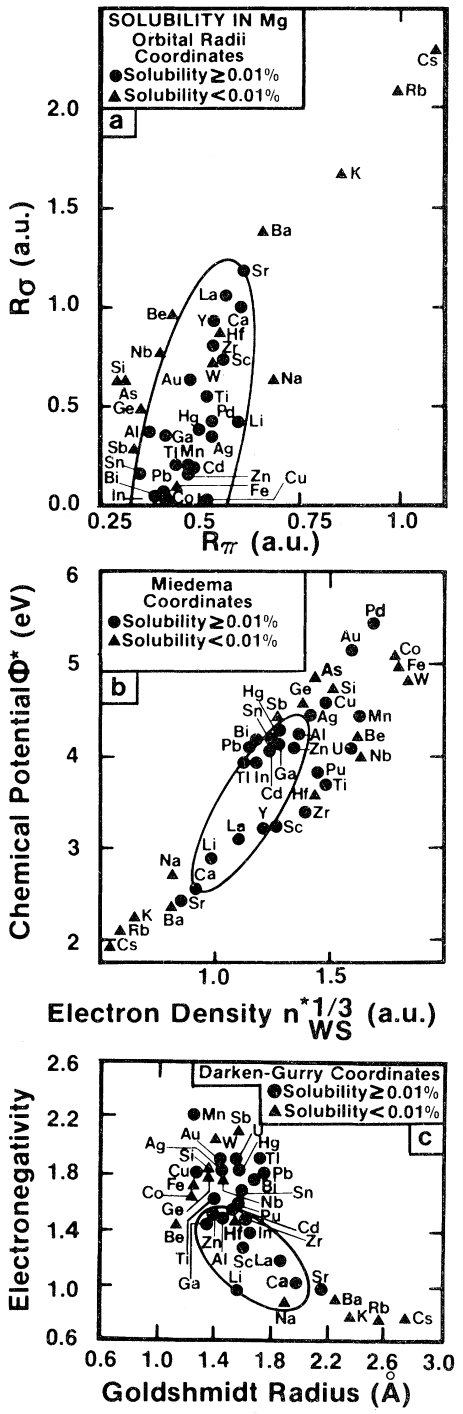

FIG. 4. Solubility map for Mg (a) using the present orbital-radii coordinates [Eq. (1)], (b) using Miedema's parameters in Chelikowsky coordinates [Eq. (3)], and (c) using the Darken-Gurry coordinates [Eq. (2)]. The data are taken at (or extrapolated to) room temperature $T_s = 300$ K (Refs. 5, 9, and 10).

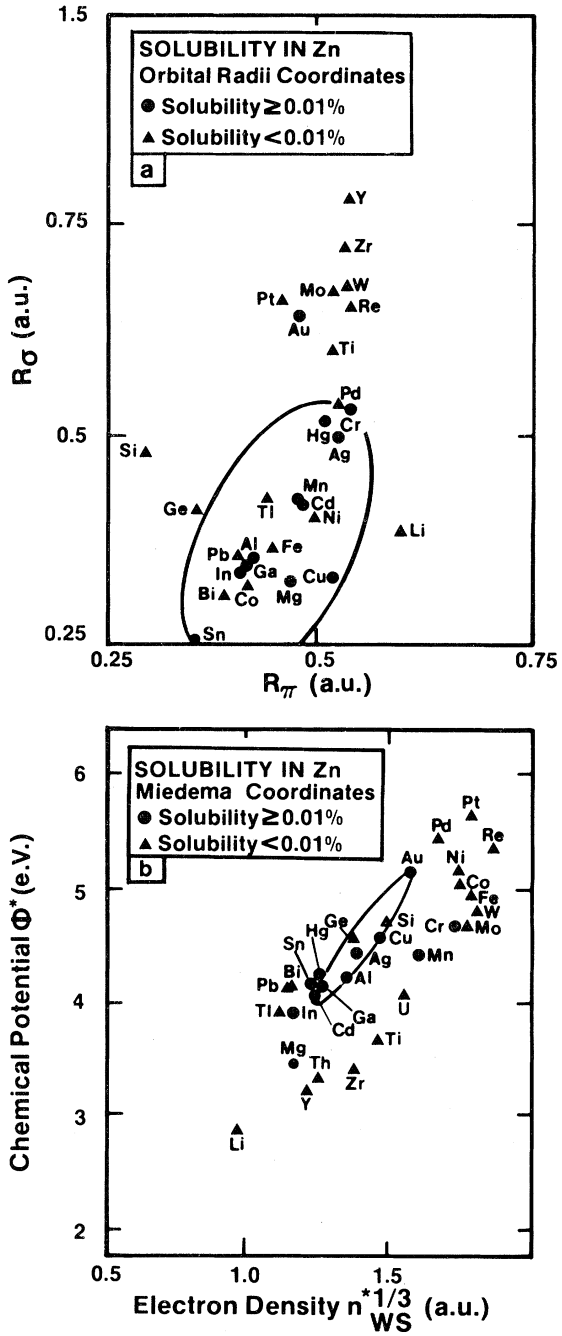

FIG. 5. Solubility map for Zn (a) using the present orbital-radii coordinates [Eq. (1)], and (b) using Miedema's parameters in the Chelikowsky coordinates [Eq. (3)]. The data is taken at (or extrapolated to) $T_s = 300$ K (Refs. 5, 9, and 10).

have sketched simple elliptical domains which include the most soluble impurities. The overall rate of "success" of the orbital-radii coordinates [Eq. (1)] over this data base of 192 data points is similar to that obtained by the empirical Miedema scale: 84%, compared with 82% using Miedema's parameters [Eq. (3)]. Given the fact that the present orbital-radii coordinates are, however, derived from first-principles and exclusively from free-atom properties (as contrasted with Miedema's parameters which are experimental and derived from data on the condensed phase), this rate of success is indeed remarkable.

Overall, the major chemical trends in the data of Table I discussed in Sec. II A are reproduced rather well. The notable features of the present results are the following.

(1) Whereas for the nonmagnetic transition-element impurities (e.g., Sc, Y, La, Ti, Zr, V, Nb, Mo, W, Mn, Pd, and Pt) the present OR coordinates are very successful (over 90% reliability), the magnetic impurities Fe, Co, and Ni are systematically predicted to be soluble in almost all of the heavier divalent hosts Mg, Cd, Zn, and Hg, in contrast with experimental results.[5,9–11] This is the only *systematic* error made by the present scheme and indicates that an explicit d-electron coordinate (i.e., r_d in Ref. 8) may be needed for these three elements. Miedema's parameters, on the other hand, make no error for the magnetic impurities but have only a rather small degree of reliability for the solubility of the other transition elements in the divalent hosts (70%).

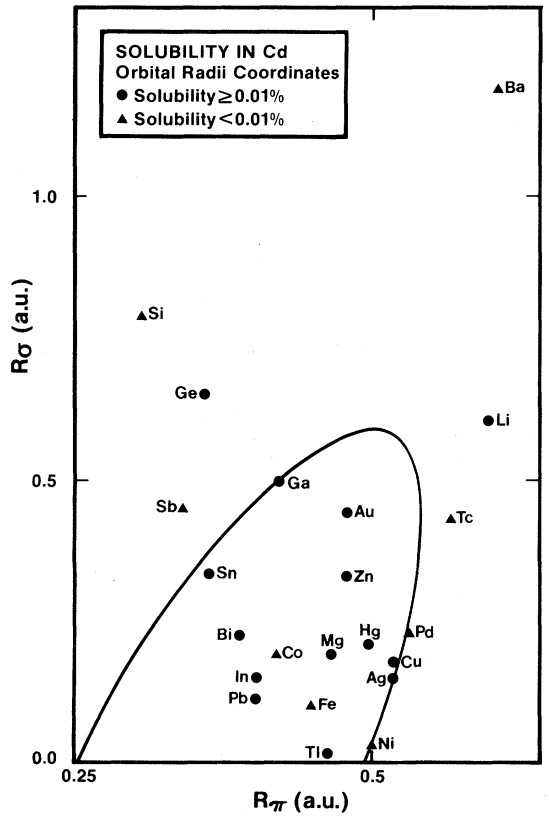

FIG. 6. Orbital-radii solubility map for Cd. The data is taken at (or extrapolated to) $T_s = 300$ K (Refs. 5, 9, and 10).

(2) For the nontransition atom impurities, the rate of success of the OR coordinates is nearly uniform throughout all columns of the Periodic Table: It ranges from 80% to 95% reliability for columns $IA-VA$ and IIB, but is only 78% for column IB. The Miedema coordinates are significantly more successful for the simple metals in columns $IA-IIIA$ (85%–100%) than they are for the nonmetals of columns $IVA-VA$ ($\sim$70%) or the post-transition-series metals of columns $IB-IIB$ (60%–70%).

(3) With the exceptions of Ag and Au in Hg, there is no overlap between the errors made by the OR coordinates and the Chelikowsky coordinates. This near independence strongly suggests that two schemes can be fruitfully combined.

(4) Comparing the metallic hosts with the covalent Si and Ge hosts, one finds that the rate of success of the OR coordinates is 80% for the former but 96% for the latter. In contrast, the Miedema parameters are comparable in predictability for the metallic hosts (82% overall reliability) but has a considerably lower predictive power (72% reliability) for the covalent hosts like Si and Ge. The higher reliability of the Miedema scheme for metals has been recognized by Chelikowsky.[5]

(5) For the divalent host crystals, the OR scheme has the highest rate of success for Mg (errors: Hf, W, Fe, and Co out of a total of 38 impurities). The Miedema parameters [Fig. 4(b)], however, show many more misplaced impurities for Mg (Sc, Cu, Au, Pb, Bi, Sr, Ti, Zr, Mn, Pu, and Pd). The Darken-Gurry parameters [Fig. 4(c)] produce yet even more misplaced impurities for this host (errors: Cu, Ag, Au, Tl, Pb, Bi, Sn, Ti, Hf, Na, Sr, Hg, and Mn). The lowest success rate for the OR coordinates occurs for the host Zn (errors: Au, Pb, Bi, Tl, Fe, Co, and Ni, out of 29 impurities). The Miedema parameters lead to a similar number of errors for this host (Mg, Hg, Sn, In, Cr, and Mn). Notice, however, that in the work of Chelikowsky the original Miedema parameters have been modified for a few elements by $\leq 5\%$; using the unmo-

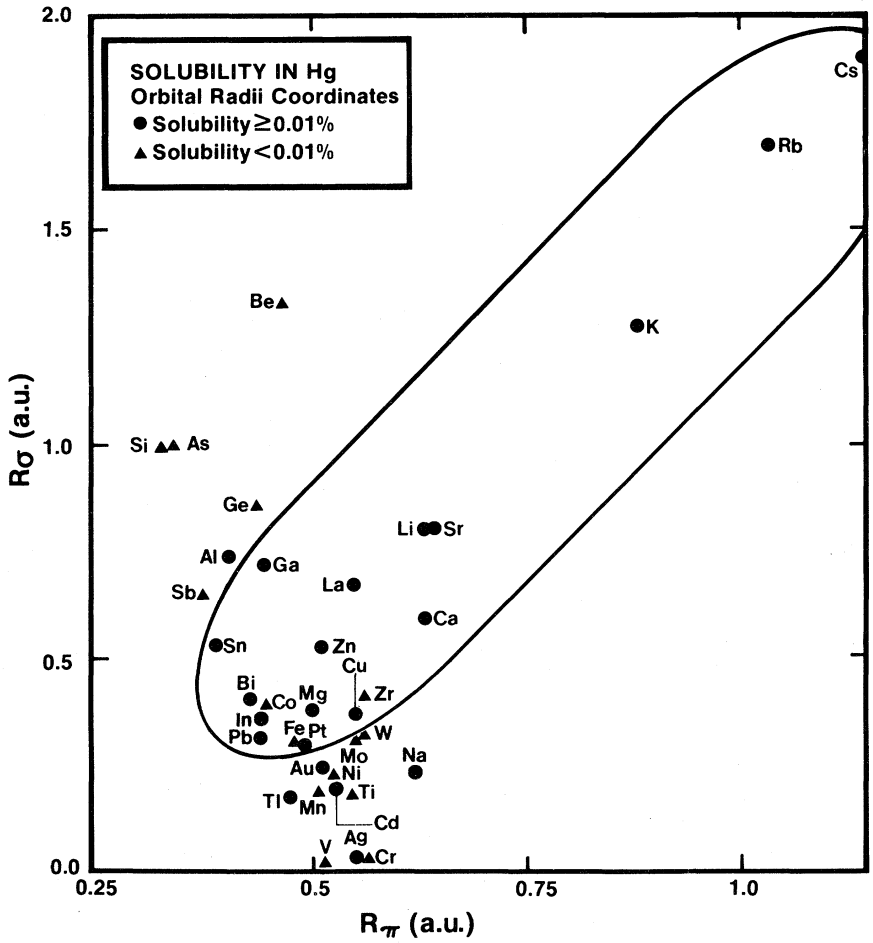

FIG. 7 Orbital-radii solubility map for Hg. The data is taken at (or extrapolated to) $T_s = 300$ K (Refs. 5, 9, and 10).

dified parameters, one finds that Al and Cd are also misplaced in Zn.

(6) It is significant that the present OR scheme is not host invariant. Whereas the $R_\pi(H,I)$ coordinate is host invariant (the relative location of various impurity atoms on this axis does not depend on the identity of the host), the $R_\sigma(H,I)$ coordinate is not. If one replaces this coordinate by the host-invariant coordinate $\hat{R}_\sigma = (r_p^I + r_s^I) - (r_p^H + r_s^H)$, (i.e., no absolute-value signs) then for the impurities with $(r_p^I + r_s^I) > (r_p^H + r_s^H)$ (e.g., Be in Hg) the $\hat{R}_\sigma$ value will be negative. This leads to a poorer separation of the soluble impurities from the insoluble impurities.

IV. AN ORBITAL-RADII APPROACH TO IMPURITY LATTICE LOCATIONS IN ION-IMPLANTED HOSTS

Ion implantation is a metastable situation. It is therefore not clear if schemes such as those of Miedema,[5,6] orbital-radii,[8] or Darken-Gurry,[2] which are based on equilibrium parameters would provide successful separations. Sood *et al.*[22] applied the Darken-Gurry scheme to the ion-implantation problem. They used a more relaxed criterion than the Hume-Rothery rules[1] to obtain separation between substitutional and nonsubstitutional implanted impurities. Kaufmann *et al.*[23] used the Miedema parameters for the Be host. The low mass of Be makes it ideal for the application of equilibrium-based schemes to metastable situations; one can study the metallurgy without interference from ballistic effects. We have applied the OR scale to classify the site location of implants in Be and Si [Figs. 3(b) and 10, respectively]. The reliability of the various schemes in correctly predicting the implant location is summarized in Tables II and III. The OR coordinates appear to be better than the Chelikowsky and Darken-Gurry coordinates.

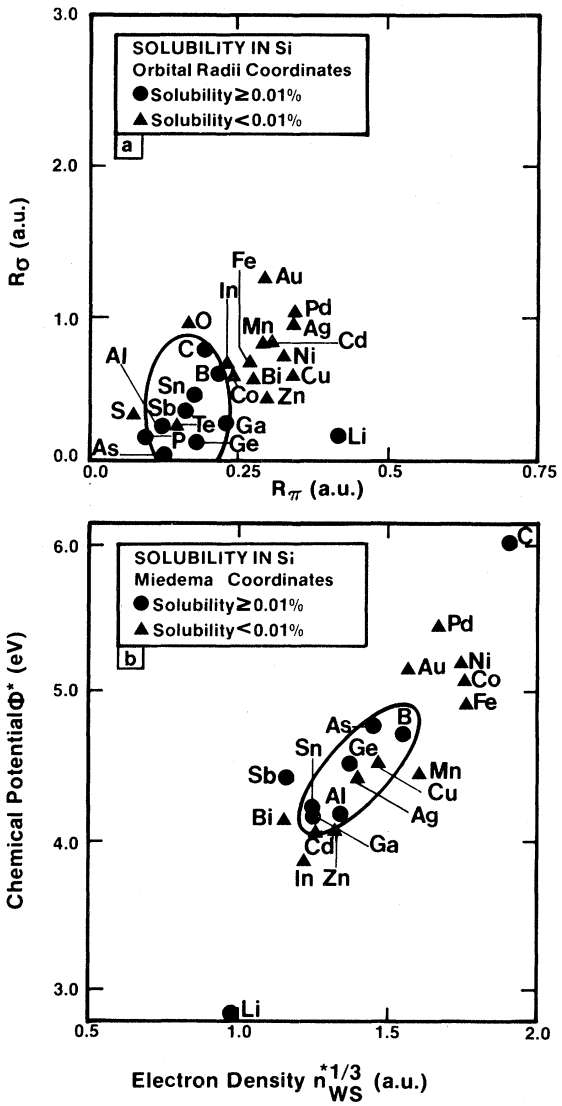

FIG. 8. Solubility map for Si (a) using the orbital-radii coordinates and (b) using Miedema coordinates [with corrections of Chelikowsky (Ref. 5)]. The data is taken at temperature $T_s = 950\,^{\circ}\mathrm{C}$ (Ref. 11).

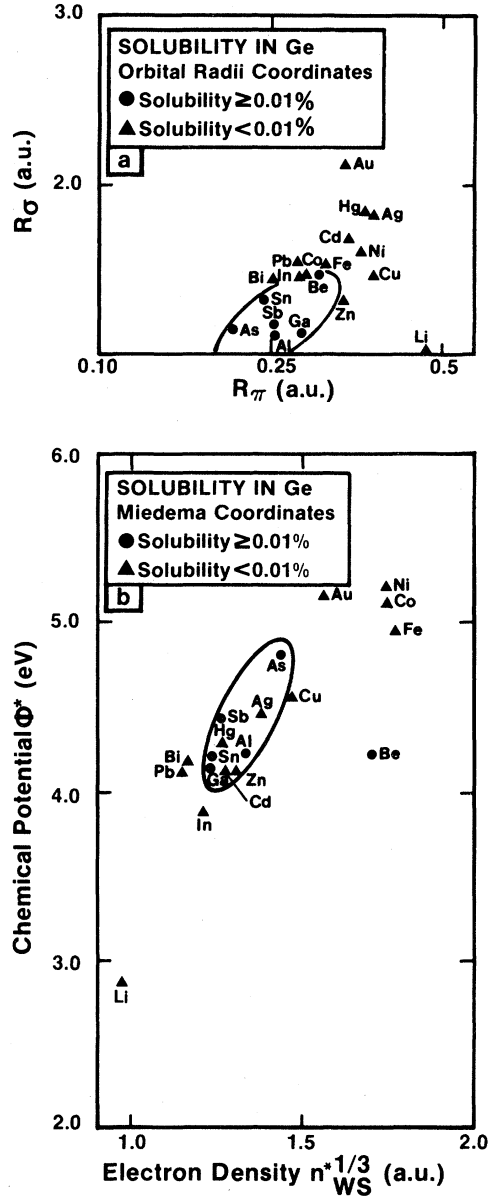

FIG. 9. Solubility map for Ge (a) using the orbital-radii coordinates and (b) using Miedema coordinates [with Chelikowsky's corrections (Ref. 5)]. The data is taken at temperature $T_s = 600\,^{\circ}\mathrm{C}$ (Ref. 11).

Figure 3(b) displays the OR plot for Be implantation. The separation of the substitutional, tetrahedral, and octahedral domains is distinct. Although not shown in the figure, Cs falls into the octahedral domain [outside the frame of Fig. 3(b)], in agreement with the experimental findings. Au and Pt are the exceptions in the substitutional case. For the tetrahedral case, In and Cd are the two exceptions. For the octahedral situation, Hg is the only exception. In a recent paper, Kaufmann *et al.*[23] suggest that Hg occupies a "displaced octahedral" site and not strictly an octahedral site.

TABLE II. Reliability of various phenomenological coordinates in predicting the location of ion-implanted impurities in Be. The total number of implants is 34.

Scheme	Substitutional (%)	Tetrahedral (%)	Octahedral (%)
Orbital radii	85	75	92
Miedema	85	69	80
Darken-Gurry	85	Does not distinguish	

A comparison reveals that OR affects a slightly better separation than Miedema scales. Experimentally, Al is a "definite interstitial" component, OR predicts an octahedral interstitial site, while the Miedema scale[5] gives it a substitutional site. For Si, OR predicts an octahedral site, while the Miedema scale places it substitutionally.[5] Both the solubility data [Fig. 3(a)] and the fact that Ge is octahedral support the OR prediction in this matter. A similar case can be made for boron: ion-implantation results oscillate between a substitutional site and a random site. The OR prediction on the substitutional-octahedral divide is more satisfactory than the strongly substitutional site predicted by the Miedema scale. That the Miedema scheme predicts Li to be nonsubstitutional[23] in conflict with experiments has been attributed to ballistic effects.[24] The OR plot depicts Li to be substitutional. Examination of Fig. 3(b) reveals that there is a lack of data points near the Li region. One could redraw the contours such that Li occupies a *special position* outside the substitutional, tetrahedral, and octahedral domains. The OR prediction for Ne (octahedral interstitial) agrees with experimental results (unspecified interstitial); however, the Miedema parameters cannot be defined for the inert gas atoms. Tables II and III rate the relative accuracy of the three schemes for experimentally monitored, implanted impurities. Table IV lists the *predictions* for Be based on the OR and Miedema scales.

For the technologically more interesting case of Si,[25] Corbett[26] unsuccessfully tried to affect a separation using the Hume-Rothery rules. We have examined the situation in detail. Figure 10 depicts the Darken-Gurry, Miedema, and OR plots for Si. For the Darken-Gurry plot [Fig. 10(c)] we have used both the Hume-Rothery rules and Sood's relaxed criterion. Table V gives the experimental data as well as the predictions of different schemes. Table III rates the relative accuracy of the various schemes. The notable features of the results for implantation in Si are the following.

(1) No element is misplaced by the OR coordinates [Fig. 10(a)], whereas the Miedema coordinates [Fig. 10(b)] place Hg, Tl, Ga, and Cd as substitutional implants and B as a nonsubstitutional implant, in conflict with the data.[25] The Darken-Gurry coordinates [Fig. (10c)] produce yet a larger number of errors (Au, Zn, Cd, Hg, Ga, Tl, and Zr).

(2) We find that in general, solubility of an impurity to a level of $X_c = 0.01$ at. % at low temperatures is a *sufficient* condition for it to be substitutional in ion implantation. If one considers the solubility data (Fig. 1), one finds that Li, As, and Ga are exceptions to this rule if the *solubility is measured at* $\sim 1000\,^{\circ}\mathrm{C}$. However, when measured at lower temperatures[11] only As and Ga seem to violate this rule. This illustrates the significance of considering low-temperature solubility data, when possible, as well as a low-threshold value of X_c (cf. discussion in Sec. II A). It is gratifying to note that both the OR and the Miedema parameters are often capable of identifying such unusual cases of soluble but interstitial impurities: As is correctly

TABLE III. Reliability of various phenomenological coordinates in predicting the location of ion-implanted impurities in Si. The total number of implants is 26.

Scheme	Substitutional (%)	Nonsubstitutional (%)
Orbital radii	100	100
Miedema	83	75
Darken-Gurry[a]	100	29
Darken-Gurry[b]	22	50

[a]Sood's criteria.
[b]Hume-Rothery criteria.

TABLE IV. Predictions for the locations of ions implanted in Be using the Miedema and OR coordinates. The notation is *O*, octahedral; *T*, tetrahedral; and *S*, substitutional. Note the different predictions for Si and Mg.

Element	Orbital radii	Miedema
Rb	*O*	*O*
K	*O*	*O*
Sr	*O*	*O*
Ca	*O*	*O-T*
Na	*O*	*O*
C	*O*	*O-S*
N	*O*	*O*
La	*T*	*T*
Y	*T*	*T*
Mg	*S*	*T*
Sc	*T*	*T*
Zr	*T*	*T*
Nb	*T*	*T*
Si	*O*	*S*
Mn	*S*	*S*
Tc	*S*	*S*
Ir	*S*	*S*
Rn	*S*	*S*

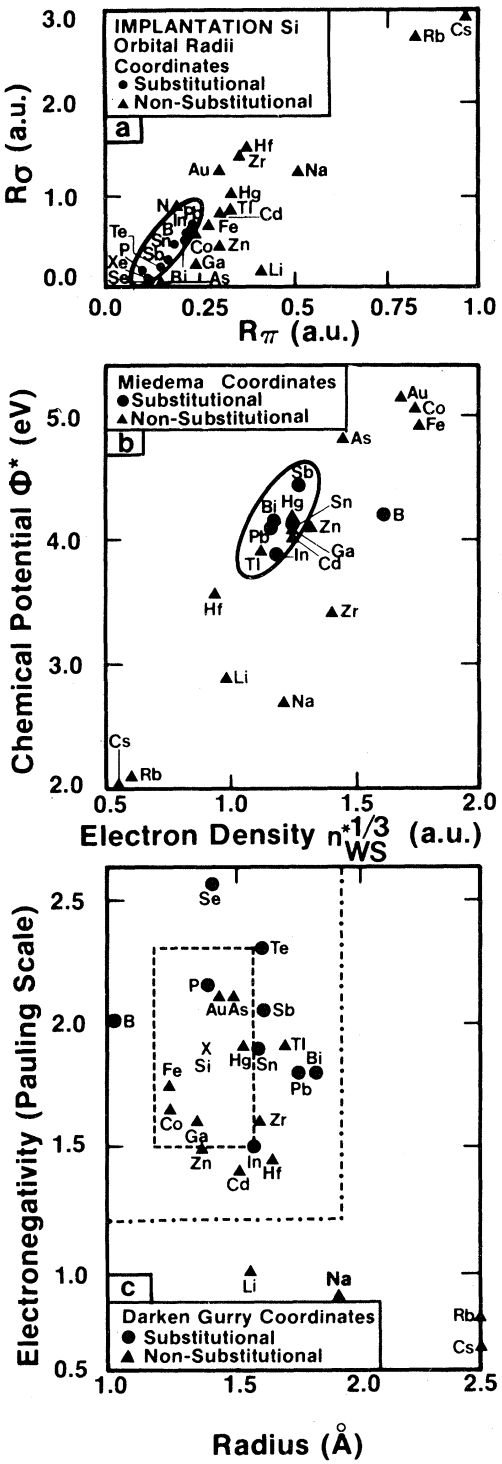

FIG. 10. Ion-implantation map for Si (a) using the present-orbital radii coordinates, (b) using the Miedema parameters, (c) using the Darken-Gurry coordinates with Hume-Rothery criteria (broken line) and Sood's criteria (dot-dashed line).

predicted by these approaches to be soluble but interstitial, while Li is predicted to be insoluble and interstitial, in agreement with the low-temperature solubility data (but not at 1000 °C) and ion implantation data. For Ga, however, the Miedema coordinates, unlike the OR coordinates and experiment, predict it to be substitutional.

(3) Solubility is not a *necessary* condition for substitutionality: In, Te, and Bi are insoluble but substitutional. Te is predicted to be soluble and substitutional, in contrast with the data showing Te to be insoluble (and substitutional). The rather old solubility data for Te may need to be reexamined to verify this point. Similarly, for Be as a host, one finds insoluble but substitutional elements such as Zn, B, and Os. In this case, however, only the OR coordinates correctly predict Zn and B to be insoluble and substitutional, whereas the Miedema coordinates predict these elements to be soluble and substitutional. The Miedema coordinates similarly predict Si and Os to be soluble (marginally for Os), while the OR coordinates correctly predict Si and Os to be insoluble. As suggested by Chelikowsky,[5] these systematic errors, characteristic of the Miedema scale, may be related to the significance of the directional forces that are absent from the isotropic Miedema coordinates. The occurrence of insoluble but substitutional implants is also known for Cu as a host[22] (Ru, Ta, Mo, and Bi are substitutional but insoluble.).

(4) Comparing the location of the ion implanted in Si with *equilibrium* data available from diffusion samples (cf. Table V) sheds some light on a few of the uncertain cases: Implantation data indicate that Li is either interstitial or random, whereas EPR experiments on equilibrated samples[27] and calculations[28] suggest it to be in a tetrahedral interstitial site, in agreement with our prediction. Similarly, for Au the channeling experiments could not clearly identify Au as substitutional or interstitial, while equilibrium data[29] indicates that it is certainly not substitutional, in agreement with our predictions; B is another case.[25] Some more examples are given in Table V. Co and Fe are also in the tetrahedral interstitial position.[31]

V. SUMMARY

The orbital-radii coordinates, derived nonempirically from a pseudopotential description of free atoms, provide a systematization of the solubility

TABLE V. Experimental (Ref. 24) data and various predictions for the ion-implantation site in Si. The symbols are *I*, interstitial; *S*, substitutional; *R*, random; *TI*, tetrahedral interstitial. Whenever experiment or theory shows a borderline case, both neighboring configurations are indicated. For comparison, we also show the solubility data (Ref. 11) at 950°C.

	Experimental			Predictions			
	Site: ion implantation	Site: equilibrium data	Solubility	OR	Miedema	Darken-Gurry [Eq. (2)]	
Impurity	(Ref. 24)	(Refs. 25–28)	(Ref. 11)	Eq. (1)	Eq. (3)	DG criteria	Sood's criteria
Li	*I,R*	*TI*[a]	+	*I*	*I*	*I*	*I*
Na	*I*			*I*	*I*	*I*	*I*
Rb	*R*			*R*	*R*	*I*	*I*
Cs	*R*			*R*	*R*	*I*	*I*
Au	*S,I*	*I*[b]	−	*I*	*I*	*S*	*S*
Zn	*I*		−	*I*	*I-S*	*S*	*S*
Cd	*I*		−	*I*	*S*	*I*	*S*
Hg	*I*			*I*	*S*	*S*	*S*
B	*S,I*	*I* near *S*[c]	+	*S*	*I*	*I*	*S*
Ga	*I*		+	*I*	*S*	*S*	*S*
In	*S*		−	*S*	*S*	*I-S*	*S*
Tl	*I*			*I*	*S*	*I*	*S*
Sn	*S*		+	*S*	*S*	*I*	*S*
Pb	*S*			*S*	*S*	*I*	*S*
N	*R*			*R*	*R*	−	−
P	*S*	*S*	+	*S*	−	*S*	*S*
As	*S,I*		+	*I*	*I*	*S*	*S*
Sb	*S*		+	*S*	*S*	*I*	*S*
Bi	*S*		−	*S*	*S*	*I*	*S*
Se	*S*			*S*	−	*I*	*S*
Te	*S*		−	*S*	−	*I*	*S*
Xe	*R,S*			*S*	−	−	−
Zr	*I*			*I*	*I*	*I*	*S*
Hf	*I*			*I*	*I*	*I*	*S*
Co	*I* near *T*	TI[d]	−	*I*	*I*	*S*	*S*
Fe	*I* near *T*	TI[d]	−	*I*	*I*	*S*	*S*

[a]References 27 and 28.
[b]Reference 29.
[c]Reference 30.
[d]Reference 31.

data (hosts Be, Mg, Zn, Cd, Hg, Si, and Ge) and the locations of ion-implantation sites (hosts Be and Si) which is equal to or better than that given by the Miedema and Darken-Gurry coordinates derived empirically from data on condensed phases. *Furthermore, the use of s and p coordinates alone [Eq. (1)] is sufficient to produce a correct systematization even for the (nonmagnetic) d-orbital transition-atom in impurities.* This supports the conclusions of Refs. 8 and 21.

We believe that the choice $X_c = 0.01$ at. % (Figs. 3–9) constitutes a stringent test. A better choice may be to plot concentric contours of decreasing solid solubility instead of committing oneself to an absolute choice.[32] Theoretical work predicting the elliptical boundaries would also be very useful.

The fact that the OR approach is nonempirical gives the scheme another advantage. OR coordi-

nates can be defined for *any* element, including group VI*A* (O,S,Se,Te,Po), group VII*A* (F,Cl,Br,I,At), and group VIII*A* (Ne,Ar,Kr,Xe,Rn) elements. Miedema coordinates do not exist for these elements. Corbett[26] has pointed out the importance of considering charged states in the study of Si implantation. OR coordinates can be calculated for elements in various charged and orbital states. This is not the case with the empirical Miedema and DG scales.

ACKNOWLEDGMENT

We thank J. W. Corbett and S. T. Picraux for very helpful and stimulating discussions. We are also grateful to J. A. Alonso, J. Chelikowsky, J. W. Corbett, L. Kaufmann, S. T. Picraux, and S. Simozar for helpful comments on the manuscript. This research was supported in part by Solar Energy Research Institute (SERI) Subcontract No. HS-0-9188-4.

[1]W. Hume-Rothery, R. E. Smallman, and C. W. Haworth, *Structure of Metals and Alloys,* 5th ed. (Institute of Metals, London, 1969).

[2]L. S. Darken and R. W. Gurry, *Physical Chemistry of Metals* (McGraw-Hill, New York, 1953)

[3]J. T. Waber, K. Gschneider, Jr., A. C. Carson, and M. Y. Prince, Trans. Metall. Soc. AIME 227, 717 (1963).

[4]K. A. Gschneider, Jr., in *Theory of Alloy Phase Formation,* edited by L. H. Bennett (The Metallurgical Society of AIME, New York, 1980), p. 1.

[5]J. R. Chelikowsky, Phys. Rev. B 19, 686 (1979).

[6]A. R. Miedema, F. R. de Boer, and P. F. de Chatel, J. Phys. F 3, 1558 (1973); A. R. Miedema, F. R. de Boer, and R. Boom, CALPHAD 1, 341 (1977); A. R. Miedema, J. Less-Common Met. 32, 117 (1973).

[7]J. A. Alonso and S. Simozar, Phys. Rev. B 22, 5583 (1980).

[8]A. Zunger, Phys. Rev. B 22, 5839 (1980); A. Zunger, Phys. Rev. Lett. 44, 582 (1980); 47, 1086 (1981).

[9]M. Hansen, *Constitution of Binary Alloys* (McGraw-Hill, New York, 1958); R. P. Elliot, *Constitution of Binary Alloys,* Suppl. 1 (McGraw-Hill, New York, 1965); F. A. Shunk, *Constitution of Binary Alloys* (McGraw-Hill, New York, 1969), Suppl. 2.

[10]W. G. Moffat, *The Handbook of Binary Phase Diagrams* (General Electric, Schenectady, New York, 1978), Vols. 1–3.

[11]F. A. Trumbore, Bell Syst. Tech. J. 39, 205 (1960).

[12]W. B. Pearson *The Crystal Chemistry and Physics of Metals and Alloys* (Wiley–Interscience, New York, 1972).

[13]D. Brust, in *Methods in Computational Physics,* edited by B. Alder, S. Fernback, and M. Rotenberg (Academic, New York, 1968), Vol. 8, p. 33; M. L. Cohen and V. Heine, in *Solid State Physics,* edited by H. Ehrenreich, F. Seitz, and D. Turnbull (Academic, New York, 1970), Vol. 24, p. 38.

[14]J. C. Phillips and J. A. Van Vechten, Phys. Rev. B 2, (1970); J. C. Phillips, Rev. Mod. Phys. 42, 317 (1970).

[15]J. St. John and A. N. Bloch, Phys. Rev. Lett. 33, 1095 (1974); E. S. Machlin, T. P. Chow, and J. C. Phillips, Phys. Rev. Lett 38, 1292 (1977); J. R. Chelikowsky and J. C. Phillips, Phys. Rev. B 17, 2453 (1978).

[16]A. Zunger and M. L. Cohen, Phys. Rev. B 18, 5449 (1978); 20, 4082 (1979).

[17]A. Zunger, Phys. Rev. B 22, 649 (1980); J. Chem. Phys. 74, 4209 (1981).

[18]L. Brewer, in *Electronic Structure and Alloy Chemistry of the Transition Elements,* edited by P. Beck (Interscience, New York, 1963), p. 221.

[19]It is intriguing to note that in the case of Fe and Co as hosts one can obtain a nearly perfect separation between soluble and insoluble impurities using only one of the Alonso-Simozar coordinates: $R_1^{AS}(I)$. One finds, for example, that in Fe as a host, most impurities having a Wigner-Seitz radius larger than ~ 3.15 a.u. are insoluble [errors: Sn and Sb, as in the two-coordinate model underlying Eq. (8)], while most impurities with $R_I^{WS} < 3.15$ a.u. are soluble (errors: B and Ag; i.e., one error more than in the two-coordinate model). Using the 12-coordinated radius[2] R_I^{CN12} [Eq. (2)] as a single scale, one finds that impurities with $R_I^{CN12} > 3$ a.u. are mostly insoluble (errors: Sb and Sn), while those with $R_I^{CN12} < 3$ a.u. are mostly soluble (errors: Ag, B, and Nb). For such hosts the $R_2^{AS}(I,H)$ coordinate is hence redundant. S. Simozar has informed us (private communication) that the $R_2^{AS}(I,H)$ coordinate is needed in the solubility plots for Cu and Ag as hosts.

[20]E. S. Machlin and S. H. Whang, Phys. Rev. Lett. 41, 1421 (1978).

[21]J. K. Burdett, G. D. Price, and S. L. Price, Phys. Rev. B 24, 2903 (1981).

[22]D. K. Sood and G. Dearnaley, in *Applications of Ion Beams in Materials,* edited by G. Carter, J. S. Colligon and W. A. Grant (IOP, London, 1976), p. 196; D. K. Sood and G. Dearnaley, Radiat. Eff. (in press).

[23]E. N. Kaufmann, R. Vianden, J. R. Chelikowsky, and J. C. Phillips, Phys. Rev. Lett 39, 1671 (1977); R. Vianden, E. N. Kaufmann, and J. W. Rodgers, Phys. Rev. B 22, 63 (1980).

[24]M. S. Duesbery and R. Taylor, J. Phys. F. 9, L19 (1979); E. N. Kaufmann, R. Vianden, T. E. Jackman, J. R. MacDonald, and L. Haggmarh, J. Phys. F. 9, L23 (1979).

[25]S. T. Picraux, *New Uses of Ion Accelerators,* edited by J. F. Ziegler (Plenum, New York, 1975), p. 229; J. C.

North and W. M. Gibson, Appl. Phys. Lett. 16, 126 (1970).

[26]J. W. Corbett, NATO A.S.I., Albany, New York, 1978 (unpublished).

[27]G. D. Watkins and F. S. Ham, Phys. Rev. B 1, 4071 (1970).

[28]Vijay A. Singh, C. Weigel, L. M. Roth, and J. W. Corbett, Phys. Status Solidi B 100, 533 (1980).

[29]Gold has been recently studied as a diffused impurity in Si [e.g., D. V. Lang, H. G. Grimmeiss, E. Meiger, and M. Jaros, Phys. Rev. B 22, 3917 (1980)]. It is certainly not substitutional.

[30]From a recent EPR experiment, Troxell and Watkins [J. R. Troxell and G. D. Watkins, Phys. Rev. B 22, 921 (1980)] concluded that the natural boron impurity is metastable in Si, whereas the charged states B^- and B^+ are located in bond-centered and split interstitial positions, respectively, the latter being close to the substitutional position.

[31]Co and Fe, as well as many other transition-atom impurities, are found both in the substitutional and the interstitial positions in Si, depending on their charged states; e.g., G. W. Ludwig and H. H. Woodbury, *Solid State Physics,* edited by F. Seitz and D. Turnbull (Academic, New York, 1962), Vol. 13, p. 263. The tetrahedral interstitial (TI) position is, however, preferred. Recent ion-implantation studies in Si place Co on the TI site and strongly suggest that Fe behaves similarly [E. Kotai, T. Lohner, A. Manuaba, G. Mezey, R. Coussement, I. Dezsi, and G. Langouche, Radiat. Eff. 47, 153 (1980)].

[32]J. A. Alonso (private communication).